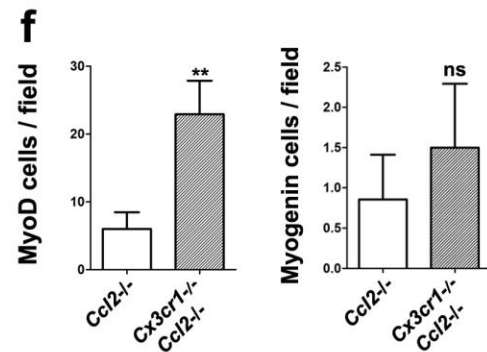
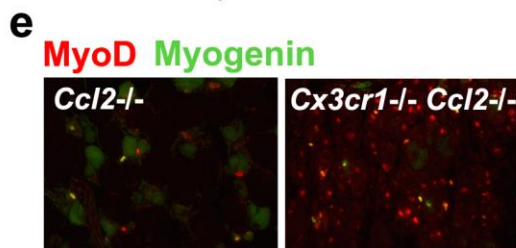
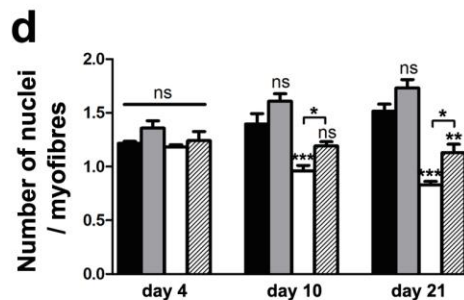
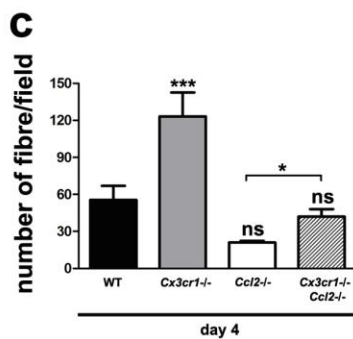
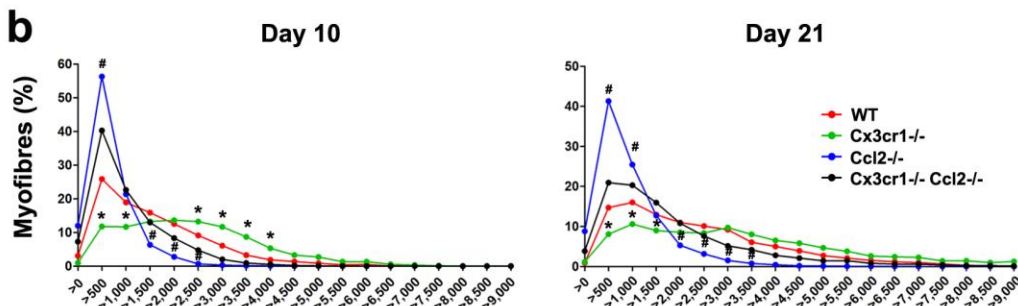
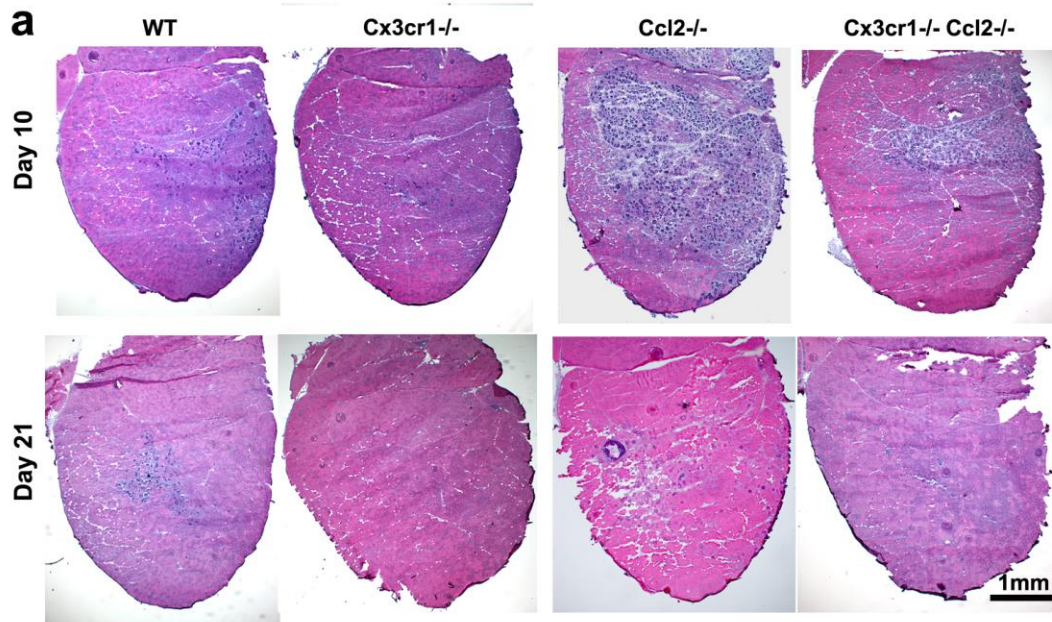


Supplementary Figure 1

Chemokine and chemokine receptor expression during muscle regeneration

(a) Analysis of CX3CR1 mRNA expression by real time-PCR at day 0, 1, 4, 10 and 21 post- muscle injury. **(b)** Mean of fluorescence intensity of GFP expression measured by flow cytometry in muscular cell suspension of *Cx3cr1^{gfp/+}* mice at day 0 (black dotted line), day 1 (green), day 4 (blue) and day 10 (red) post-injury (one representative experiment out of 3) **(c)** CX3CL1 and **(d)** CCL2 proteins detection by ELISA on muscle tissue lysates extracted at days 0, 1, 4, 10 and 21 post-injury. Data are mean + s.e.m. of 3 to 4 mice per time point in 2 to 4 distinct experiments. * $p < 0.05$ and *** $p < 0.001$ for each time point versus day 0.

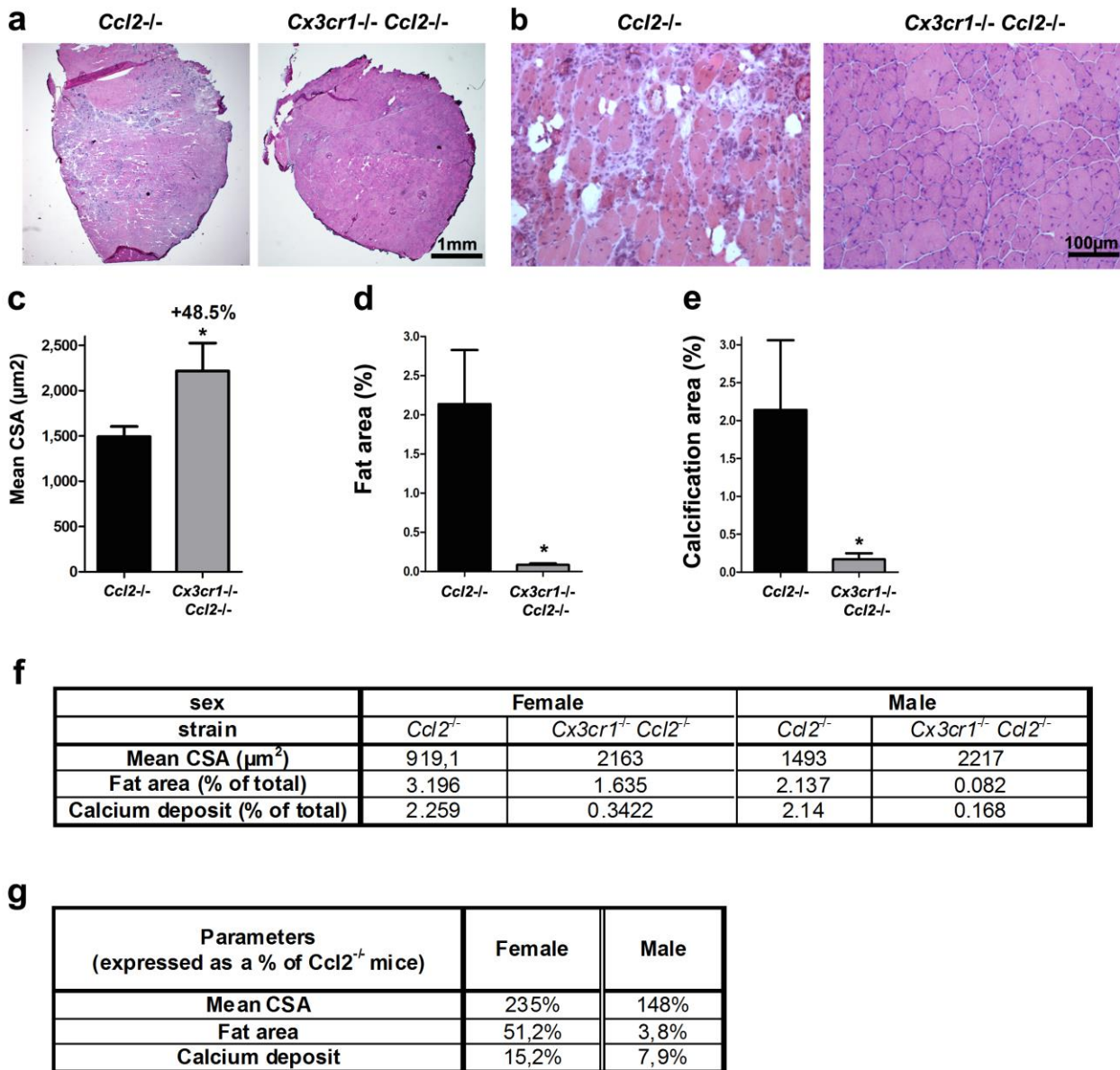


Supplementary Figure 2

Muscle regeneration in WT, Cx3cr1^{-/-}, Ccl2^{-/-} and Cx3cr1^{-/-} Ccl2^{-/-} mice

(a) Representative whole muscle cross-section of injured muscle from WT, Cx3cr1^{-/-}, Ccl2^{-/-} and Cx3cr1^{-/-} Ccl2^{-/-} mice on days 10 and 21 post-injury. (b) Distribution of CSA of regenerating myofibres

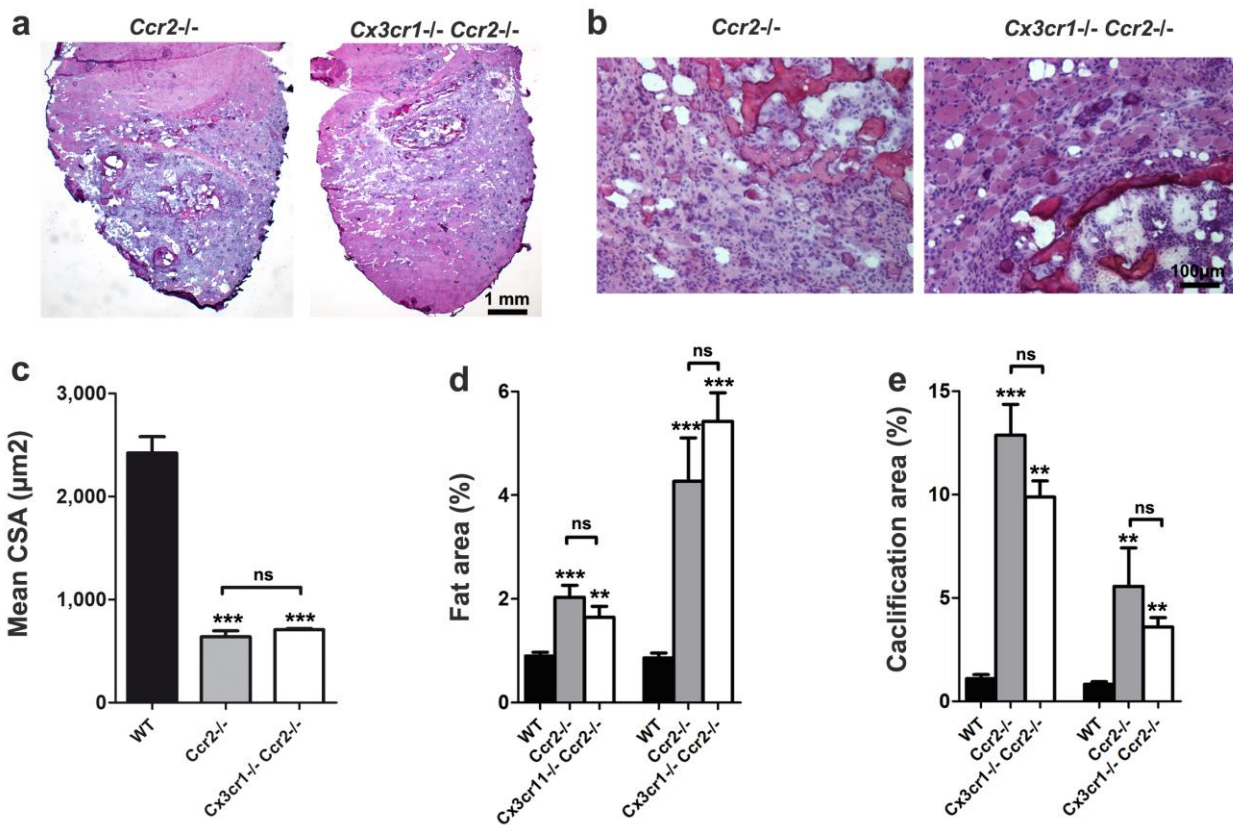
for each mouse strain on days 10 and 21 post-injury. Data are means + s.e.m. of 6 mice per strain in 2 distinct experiments. * $p < 0.05$ for *Cx3cr1*^{-/-} strain versus wild-type and # $p < 0.05$ for *Ccl2*^{-/-} versus *Cx3cr1*^{-/-} *Ccl2*^{-/-} strains. **(c)** Quantification of the total number of regenerating myofibres per field on day 4 post-injury. Data are means + s.e.m. of at least 3 different fields taken from 6 different mice per strain. **(d)** Number of myonuclei inside regenerating myofibres divided by the total number of regenerating myofibres on day 4 post-injury. Data are means + s.e.m. of at least 3 different fields taken from 6 different mice per strain. **(e)** Example of muscle cross-sections of *Ccl2*^{-/-} and *Cx3cr1*^{-/-} *Ccl2*^{-/-} mice immunolabelled with MyoD (red) and myogenin antibodies (green) on day 4 post-injury. **(f)** Quantification of MyoD-positive and myogenin-positive cells in an average of 5 fields per mouse on day 4 post-injury (magnification of x40). Data are mean + s.e.m. of 2 different mice per strain. ns: not significant, * $p < 0.05$, ** $p < 0.01$ and *** $p < 0.001$ for each knock-out strain versus WT and for *Ccl2*^{-/-} versus *Cx3cr1*^{-/-} *Ccl2*^{-/-} mice.



Supplementary Figure 3

Analysis of muscle regeneration in male and female *Ccl2*^{-/-} and *Cx3cr1*^{-/-} *Ccl2*^{-/-} mice

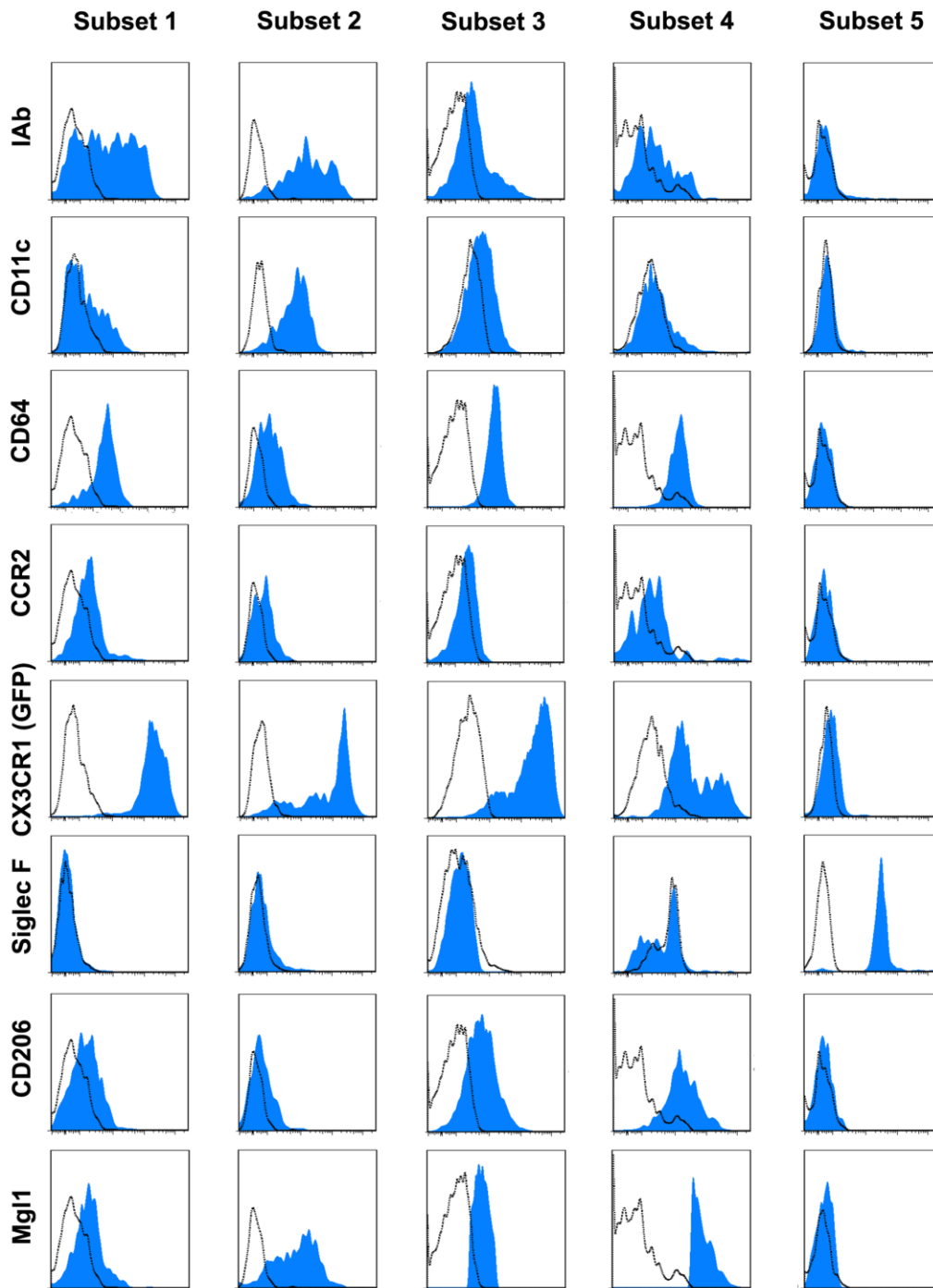
(a) Representative whole muscle cross-sections on day 21 post-injury of *Ccl2*^{-/-} and *Cx3cr1*^{-/-} *Ccl2*^{-/-} male mice. (b) 100x magnification of representative injured muscle of *Ccl2*^{-/-} and *Cx3cr1*^{-/-} *Ccl2*^{-/-} male mice. (c-e) Quantification of muscle regeneration, by measurement of the mean CSA of regenerating myofibres (c), and the areas of fat (d) and calcification (e). Results are mean + s.e.m. of 4 mice per group. (f, g) Comparison of muscle regeneration between *Ccl2*^{-/-} and *Cx3cr1*^{-/-} *Ccl2*^{-/-} female/male mice on day 21 post-injury, expressed as absolute values (f) and percentages (g).



Supplementary Figure 4

Analysis of muscle regeneration in *Ccr2*^{-/-} and *Cx3cr1*^{-/-} *Ccr2*^{-/-} mice

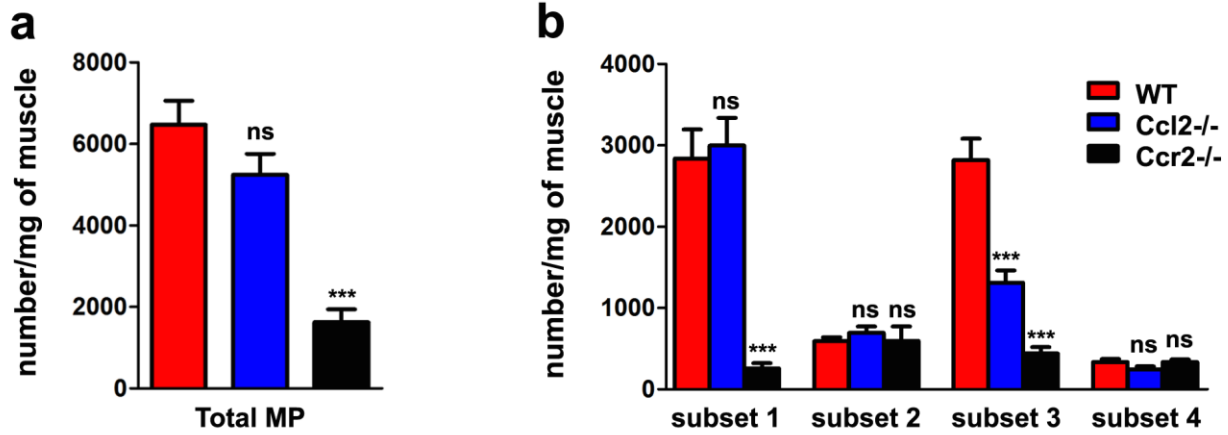
(a) Representative whole muscle cross-sections on day 21 post-injury of *Ccr2*^{-/-} and *Cx3cr1*^{-/-} *Ccr2*^{-/-} female mice. (b) 100 \times magnification of representative injured muscle of *Ccr2*^{-/-} and *Cx3cr1*^{-/-} *Ccr2*^{-/-} mice. (c-e) Quantification of muscle regeneration by measurement of the mean CSA of regenerating myofibres (c), and areas of fat (d) and calcification (e). Results are mean + s.e.m. of 3 mice per group. ns: not significant, * $p < 0.05$, ** $p < 0.01$ and *** $p < 0.001$ for each knock-out strain versus WT mice.



Supplementary Figure 5

Phenotypic characterization of mononuclear phagocytes in injured muscle of WT mice

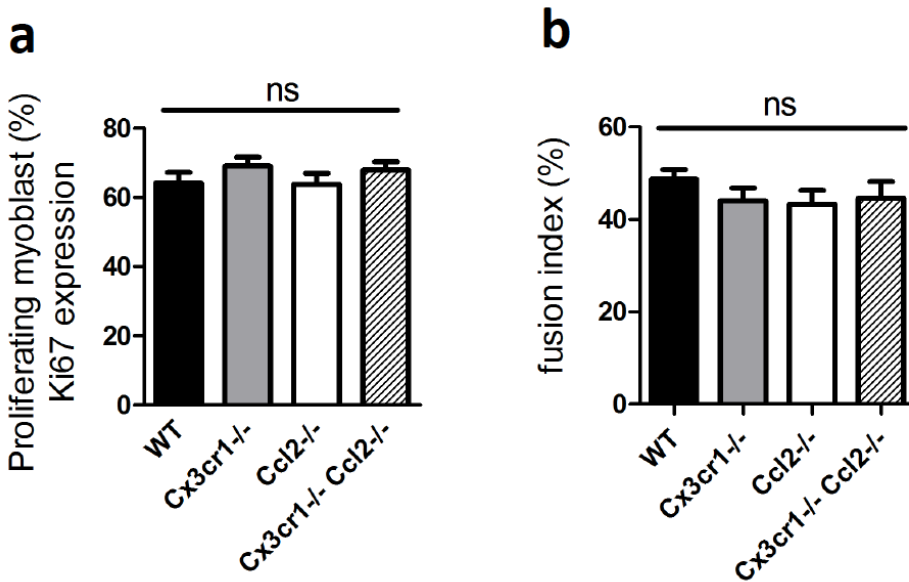
Cells were been sorted from injured muscles of WT mice on day 4 post-injury after enzymatic digestion and analysed for various surface markers by flow cytometry. Subsets 1, 2, 3 and 4 of MPs identified in Figure 3 as well as F4/80⁺ CD11b⁺ Mgl1⁻ cells corresponding to eosinophils were stained with haematoxylin/eosin and tested for expression of IAb (major histocompatibility complex (MHC) molecules - class II), CD11c, CD64, CCR2, CX3CR1, Siglec F, CD206 and Mgl1. Histograms of 1 representative experiment out of 3.



Supplementary Figure 6

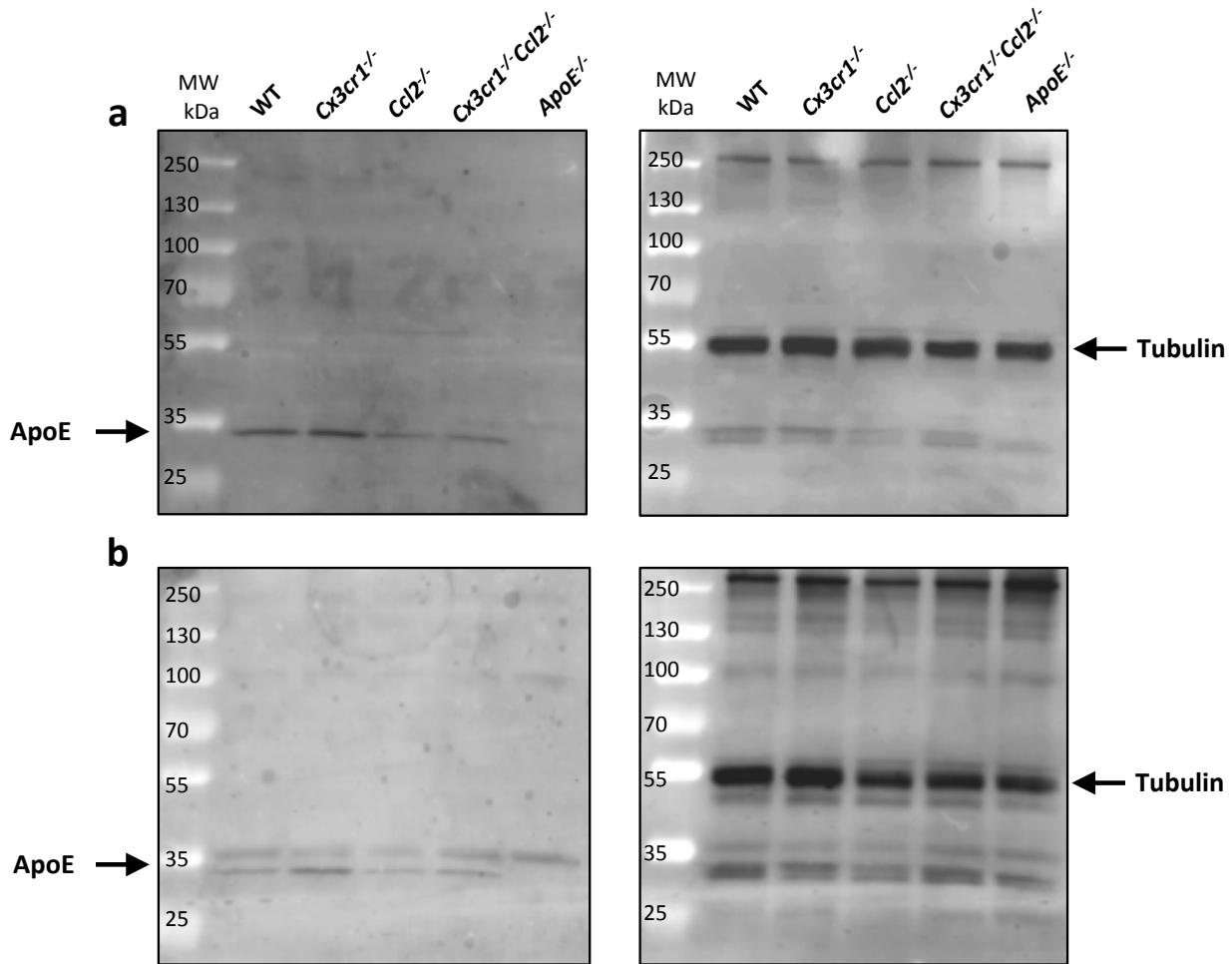
Mononuclear phagocyte distribution 4 days post-injury in *Ccl2*^{-/-} and *Ccr2*^{-/-} mice

(a) Total number and **(b)** number per subset of MPs extracted from injured muscles of WT (*n*=12), *Ccl2*^{-/-} (*n*=12) and *Ccr2*^{-/-} (*n*=4) mice. ns: not significant, *** *p*<0.001 for each knock-out strain versus WT mice.



Supplementary Figure 7
Macrophages effect toward myogenesis

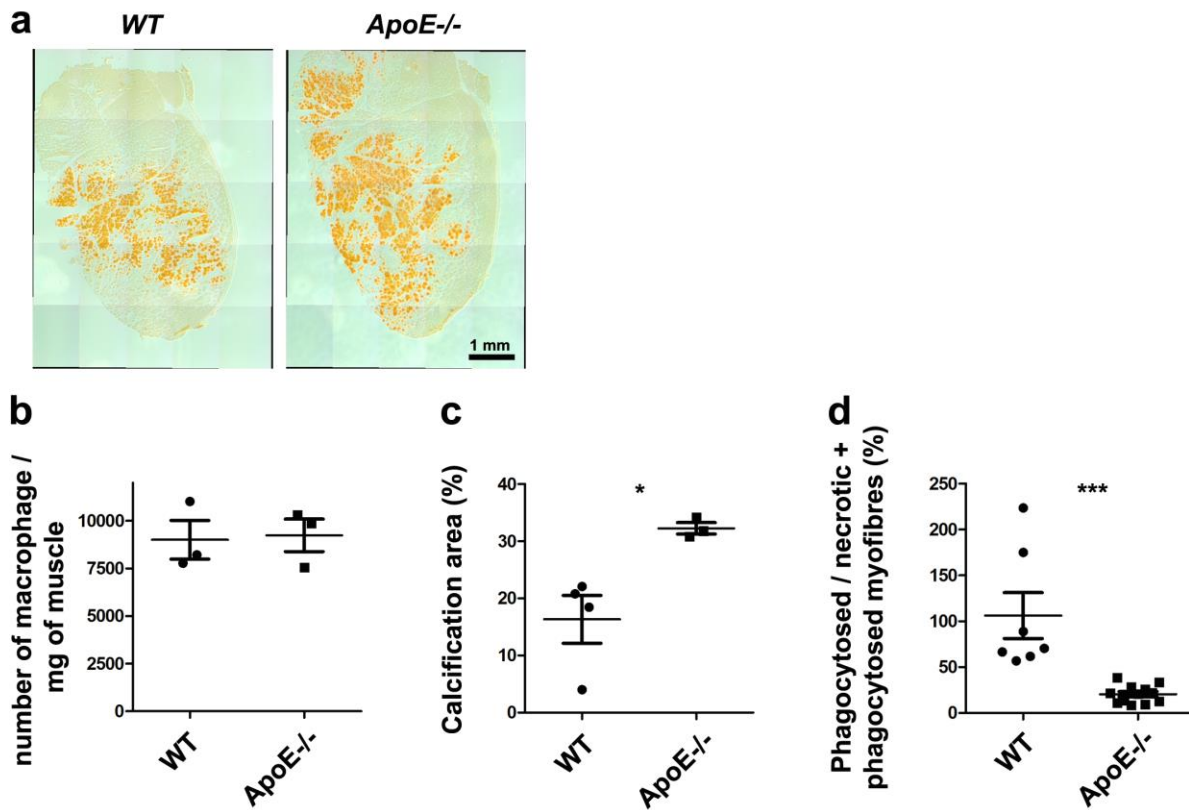
In vitro experiments have been performed to understand the role of CX3CR1 and CCL2 expressing macrophage toward myogenic precursor cells proliferation (Ki67 expression) and fusion (% of myoblast within myotubes vs total number of myoblast counted). **(a)** 24h conditioned media from WT, Cx3cr1^{-/-}, Ccl2^{-/-} and Cx3cr1^{-/-} Ccl2^{-/-} bone marrow derived macrophages have been added on primary myogenic precursor cells and the Ki67 expression has been assessed 1 day later. **(b)** Myoblast fusion index has been assessed 4 days after macrophage conditioned media addition. Results are a mean + s.e.m. of 2 distinct experiments. ns: not significant



Supplementary Figure 8

ApoE expression in mononuclear phagocytes from injured muscle of WT, *Cx3cr1*^{-/-}, *Ccl2*^{-/-} and *Cx3cr1*^{-/-}*Ccl2*^{-/-} mice

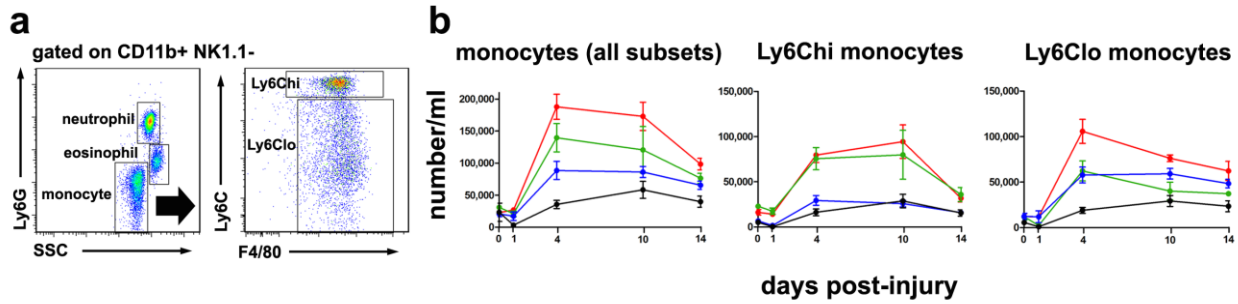
Mononuclear phagocytes were isolated from muscle of WT, *Cx3cr1*^{-/-}, *Ccl2*^{-/-}, *Cx3cr1*^{-/-}*Ccl2*^{-/-} and *ApoE*^{-/-} mice 4 days post-notexin injection using magnetic columns (CD11b+ Ly6G- NK1.1-). Western-blots (45µg of total protein/lane) were performed using antibodies against ApoE (left panel) and against tubulin (right panel) from 2 independent experiments (a and b) (First lane: Molecular weight (MW) indicated in kDa).



Supplementary Figure 9

Necrotic/calcified myofibres removal by mononuclear phagocytes in ApoE^{-/-} mice

(a) Representative whole muscle cross-sections on day 4 post-injury of WT and ApoE^{-/-} female mice stained with Alizarin Red. (b) Total number of MPs extracted from injured muscles of WT (n=3) and ApoE^{-/-} (n=3) mice. Quantification of muscle debris removal by assesment of the calcification area (n=3 mice per strain) (c) as well as the percentage of phagocytosed vs necrotic myofibres (d) on day 4 post-injury. WT (n=7) and ApoE^{-/-} (n=10) mice. Results are a mean + s.e.m. of 2 distinct experiments. ns: not significant, *p<0.05 and *** p<0.001 for ApoE^{-/-} mice versus WT mice.



Supplementary Figure 10

Kinetics of blood monocytosis during skeletal muscle regeneration

Blood was collected in heparin, labelled with Ly6G, CD11b, F4/80, NK1.1 and Ly6C antibodies and analysed by flow cytometry. **(a)** The two subsets of blood monocytes are identified as CD11b⁺ F4/80⁺ Ly6G⁻ NK1.1⁻ SSC^{low} cells according to the expression level of Ly6C antigen. Ly6C^{high} monocytes correspond to the so-called inflammatory monocytes whereas Ly6C^{low} monocytes correspond to patrolling MOs. **(b)** Kinetics of blood monocytes depicted as total number and number of Ly6C^{high} and Ly6C^{low} monocytes during muscle regeneration in WT (red line), *Cx3cr1* (green line), *Ccl2* (blue line) and *Cx3cr1 Ccl2* (black line) -deficient mice. Data are mean + s.e.m. of at least 6 mice per strain and per time point in 2 to 4 distinct experiments.